MEBT2 PHYSICS DESIGN FOR THE C-ADS LINAC

Zhen Guo, Huiping Geng, Jingyu Tang, Zhihui Li, IHEP, Beijing, China

Abstract

The C-ADS linac is composed of two parallel injectors and a main linac, a section of Medium Energy Beam Transport (MEBT2) is designed to guide and match beams from the two injectors to the main linac. The two injectors are hot-spare for each other in order to meet the requirement of very high availability and reliability. At 10 MeV and 10 mA, with strong space charge effects and bending sections, it is found that MEBT2 design is a real challenge.. It is difficult to obtain satisfactory longitudinal matching without bunchers in the bending section, whereas bunchers in a bending section destroy usual achromatism conditions. A special design with bunchers inside the bending section is proposed, which can maintain the achromatism. The online and offline operation modes for each injector have been considered in the MEBT2 design. The multi-particle simulations have also been given.

LAYOUT DESIGN FOR MEBT2

The C-ADS accelerator is a CW proton linac and uses superconducting acceleration structures except the RFQs, the design specifications for the proton beam are shown in Table 1[1]. The C-ADS linac requires two injectors as each of them is a hot-spare of the other [1]. As this is a high-intensity beam, the physics design of the MEBT2 is tightly constrained by the requirement of very strict control over beam loss and emittance growth. Due to relatively low beam energy of 10 MeV and high intensity of 10 mA, space charge forces are strong here. To avoid significant emittance growth, it is preferred to design a lattice with more-or-less uniform focusing [2]. However, a minimum separation in the transverse space between the two injectors requires a bending section for each branch. It is not easy to maintain the focusing uniformity together with an achromatic bending. A larger bending angle is favored to give more installation space for the injectors, but it increases the difficulty to obtain a good performance in beam dynamics with high-intensity. At the moment, a trade-off design defines 2.4 m for the minimum translational separation between the two injectors. Hence an anti-symmetric bending section of 20° is employed here. Once in the straight main linac tunnel, the elements are common for operating any injector.

The most difficult problem in designing MEBT2 is the longitudinal matching. On the one hand, even at the energy of 10 MeV the required RF voltage for the bunchers is quite high, On the other hand, the RF voltage may be somewhat too low for adopting a superconducting structure and a superconducting cavity together with its cryomodule will take large longitudinal space that is not desired in the MEBT2 design. To solve this problem, we have investigated the possibility to use room-temperature cavities in 650 MHz by taking the advantage of higher focusing gradient with higher RF frequency. However, the study shows that in the CW mode a cavity in 650 MHz even with a half voltage is more difficult to cool than the one in 325 MHz. Therefore, we decide just to use more cavities of 325 MHz when higher voltage is needed.

Table 1: Specifications of the Required Proton Beams for C-ADS

Particle	**Proton**	
Energy	1.5	GeV
Current	10	mA
Beam power	15	MW
RF frequency	(162.5)/325/650	MHz
Duty factor	100	%
Beam Loss	<1	W/m
Beam trips/year	<25000	1s<t<10s
	<2500	10s<t<5m
	<25	t>5m

For the positions of the room-temperature bunchers, it is a critical issue in the MEBT2 design. With a long drift distance and in the presence of space charge force at 10 mA, the debunching process is very strong. It is found that it is difficult to obtain satisfactory longitudinal matching without bunchers in the bending section. Then we consider designing the bending section with two or more bunchers inside, the condition of maintaining the achromatism will be discussed below.

The bending section consists of three parts: the first bend magnet, the beam line between the two bending magnets which comprises quadrupoles and bunchers and the second bending magnet. Their transfer matrixes can be expressed as

$$B = \begin{pmatrix} B_{11} & B_{12} & 0 & 0 & 0 & B_{16} \\ B_{21} & B_{22} & 0 & 0 & 0 & B_{26} \\ 0 & 0 & 1 & B_{34} & 0 & 0 \\ 0 & 0 & 0 & 1 & 0 & 0 \\ -B_{26} & -B_{16} & 0 & 0 & 1 & B_{56} \\ 0 & 0 & 0 & 0 & 0 & 1 \end{pmatrix}$$

$$R = \begin{pmatrix} R_{11} & R_{12} & 0 & 0 & 0 & 0 \\ R_{21} & R_{22} & 0 & 0 & 0 & 0 \\ 0 & 0 & R_{33} & R_{34} & 0 & 0 \\ 0 & 0 & R_{43} & R_{44} & 0 & 0 \\ 0 & 0 & 0 & 0 & R_{55} & R_{56} \\ 0 & 0 & 0 & 0 & \boldsymbol{R_{65}} & R_{66} \end{pmatrix}$$

ISBN 978-3-95450-118-2

$$B' = \begin{pmatrix} B'_{11} & B'_{12} & 0 & 0 & 0 & B'_{16} \\ B'_{21} & B'_{22} & 0 & 0 & 0 & B'_{26} \\ 0 & 0 & 1 & B'_{34} & 0 & 0 \\ 0 & 0 & 0 & 1 & 0 & 0 \\ -B'_{26} & -B'_{16} & 0 & 0 & 1 & B'_{56} \\ 0 & 0 & 0 & 0 & 0 & 1 \end{pmatrix}$$

The transfer matrix of the whole bending section is

$$M = B' \cdot R \cdot B$$

The eight elements related to transverse-longitudinal coupling can be expressed as

$$M_{15} = B'_{16} \cdot \boldsymbol{R_{65}} \qquad M_{25} = B'_{26} \cdot \boldsymbol{R_{65}}$$

$$M_{61} = -B_{26} \cdot \boldsymbol{R_{65}} \qquad M_{62} = -B_{16} \cdot \boldsymbol{R_{65}}$$

$$M_{16} = B_{16} \cdot (R_{11} \cdot B'_{11} + R_{21} \cdot B'_{12}) + B_{26} \cdot (R_{12} \cdot B'_{11} + R_{22} \cdot B'_{12}) + B_{56} \cdot \boldsymbol{R_{65}} \cdot B'_{16} + \boldsymbol{R_{66}} \cdot B'_{16}$$

$$M_{26} = B_{16} \cdot (R_{11} \cdot B'_{21} + R_{21} \cdot B'_{11}) + B_{26} \cdot (R_{12} \cdot B'_{21} + R_{22} \cdot B'_{11}) + B_{56} \cdot \boldsymbol{R_{65}} \cdot B'_{26} + \boldsymbol{R_{66}} \cdot B'_{26}$$

$$M_{51} = -B'_{16} \cdot (R_{22} \cdot B_{21} + R_{21} \cdot B_{11}) - B'_{26} \cdot (R_{12} \cdot B_{21} + R_{11} \cdot B_{11}) - B'_{56} \cdot \boldsymbol{R_{65}} \cdot B_{26} - \boldsymbol{R_{55}} \cdot B_{26}$$

$$M_{52} = -B'_{16} \cdot (R_{22} \cdot B_{11} + R_{21} \cdot B_{12}) - B'_{26} \cdot (R_{12} \cdot B_{11} + R_{11} \cdot B_{12}) - B'_{56} \cdot \boldsymbol{R_{65}} \cdot B_{16} - \boldsymbol{R_{55}} \cdot B_{16}$$

Because of the existence of bunchers the element $\mathbf{R_{65}}$ of transfer matrix R may be not zero and this will bring some difficulties in maintaining the achromatism. To decouple the transverse-longitudinal coupling, elements M_{15}, M_{25}, M_{61} and M_{62} should be zero, this means we should properly set the bunchers and make sure that $\mathbf{R_{65}}$ is zero.

Without loss of generality, we can assume that we have two bunchers inside the bending section and their longitudinal transfer matrixes are

$$V = \begin{pmatrix} 1 & 0 \\ v & 1 \end{pmatrix} \qquad U = \begin{pmatrix} 1 & 0 \\ u & 1 \end{pmatrix}$$

The longitudinal transfer matrixes of beam lines before, between and behind the two bunchers can be expressed as

$$L_1 = \begin{pmatrix} 1 & l_1 \\ 0 & 1 \end{pmatrix} \quad L_2 = \begin{pmatrix} 1 & l_2 \\ 0 & 1 \end{pmatrix} \quad L_3 = \begin{pmatrix} 1 & l_3 \\ 0 & 1 \end{pmatrix}, \text{ and}$$

$$\begin{pmatrix} R_{56} & R_{56} \\ R_{65} & R_{66} \end{pmatrix} = L_3 \cdot U \cdot L_2 \cdot V \cdot L_3$$

$$= \begin{pmatrix} v \cdot (l_3 + l_2 \cdot (u \cdot l_3 + 1)) + u \cdot l_3 + 1 & l_3 + l_2 \cdot (u \cdot l_3 + 1) + l_1 \cdot (v \cdot (l_3 + l_2 \cdot (u \cdot l_3 + 1)) + u \cdot l_3 + 1) \\ u + v \cdot (u \cdot l_2 + 1) & l_1 \cdot (u + v \cdot (u \cdot l_2 + 1)) + u \cdot l_2 + 1 \end{pmatrix}$$

Then $\boldsymbol{R_{65}}$ of transfer matrix R becomes

$$\boldsymbol{R_{65}} = u + v \cdot (u \cdot l_2 + 1)$$

If we assume that the two bunchers are the same, which means v=u. When $\boldsymbol{R_{65}}$ is zero, we can obtain

$$v \cdot l_2 = -2$$

$$\begin{pmatrix} R_{56} & R_{56} \\ R_{65} & R_{66} \end{pmatrix} = \begin{pmatrix} -1 & -l_1 + l_2 - l_3 \\ 0 & -1 \end{pmatrix}$$

In the case of MEBT2, the two bending magnets are the same except the deflection direction, then

$$B_{16} = -B'_{16} \qquad B_{26} = -B'_{26}$$

After carefully studying elements M_{15}, M_{25}, M_{61}, M_{62}, M_{16}, M_{26}, M_{51} and M_{52} of transfer matrix M again, we can conclude that with two bunchers of the same voltage in the bending section the achromatism can be maintained if the effective voltage is inversely proportional to the distance between the two bunchers and at the same time one changes the original anti-symmetric focusing structure to a symmetric one.

Given that a 325-MHz buncher cannot deliver RF voltage higher than 120 kV in the CW mode, it is not easy to find a solution with this compact bending section. Finally, we are able to obtain a reasonable solution with four bunchers in the bending section, where a pair is placed close to the first bending magnet and another pair close to the second bending magnet. The distance between the two bunchers in each pair is quite short compared with the distance between the two pairs, and to some extent we can consider each pair of bunchers as a buncher with doubled voltage.

For each injector, the beam will be directed to the main linac through the main line of the MEBT2 when it is turned into the online operation mode, and the beam will be directed to a beam dump through an auxiliary beam line when it is in the offline mode. The dump line is also used for the commissioning or beam setup of the injector. The layout of a preliminary design is shown in Figure 1.

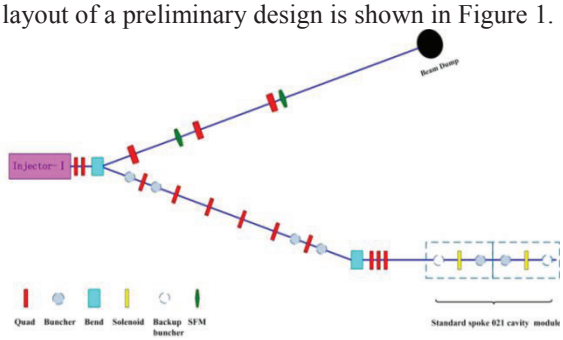

Figure 1: Layout of MEBT2 (only the upper part of two symmetric branches is shown).

For each of the mainstream lines of the MEBT2, eight quadrupoles, two bending magnets and four bunchers are used. The design scheme satisfies the requirements of more-or-less uniform transverse focusing, achromatic bending and good control in the beam phase width. In the common part, three quadrupoles, two Spoke021 cavities and two solenoids are used for the matching in the phase spaces.

Beam diagnostics in MEBT2 is also very important for commissioning and beam tuning, thus sufficient spaces have to be reserved for installing diagnostic device. It is also under consideration if and how a beam collimation will be implanted in MEBT2. It is considered possible to perform some kind of longitudinal collimation by placing collimators in the dispersive region. The sparse longitudinal halo from the RFQ is considered to be one of the important beam loss sources at higher energy part of the linac, and should be removed in MEBT2 if possible. The optimization of the MEBT2 will continue.

The evolutions of the beam envelopes along the MEBT2 are shown in Figure 2 by TraceWin [3]. The main parameters of the elements are listed in Table 2.

ISBN 978-3-95450-118-2

MULTI-PARTICLE SIMULATION RESULTS

The rms beam sizes in both the transverse and longitudinal planes along the MEBT2 are shown in Figure 2. The input beam parameters used in the simulations are: beam energy E=10 MeV, Gaussian distribution truncated to ±3σ, rms normalized transverse emittance x=y=0.206 πmm.mrad, rms normalized longitudinal emittance z=0.166 πmm.mrad, and the beam current I=10 mA.

The number of particles used for multi-particle tracking is 100000. The distributions at the MEBT2 entrance and MEBT2 exit are shown in the upper plots and lower plots in Figure 3, respectively. The ellipses in the plots also denote the fit emittance with 99% particles included. We can see that after passing through the MEBT2 line, the transversal distributions are still basically Gaussian, although a few halo particles are recognizable around the beam core. In the longitudinal phase plane, the distribution is more distorted due to the nonlinear space charge force and longer drifts between focusing elements.

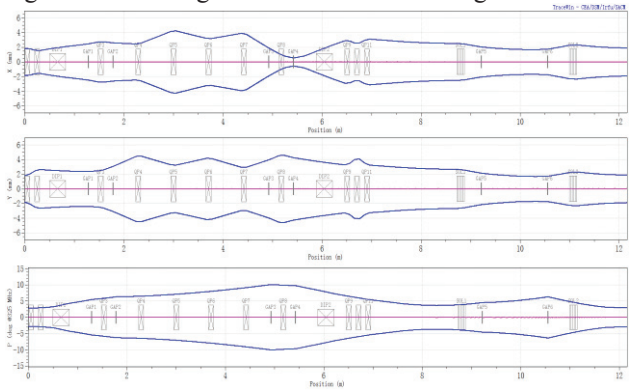

Figure 2: Evolutions of the rms beam size along the MEBT2.

Table 2: Main Parameters of the MEBT2 Elements

Element	Length (mm)	Bore radius /Half aperture (mm)	Field gradient (T/m) / Effective voltage (kV) /Field (T)
Bend-1	327	20	0.5
Bend-2	327	20	0.5
Q1	100	30	7.32
Q2	100	30	-8.30
Q3	100	30	3.60
Q4	100	30	-5.09
Q5	100	30	4.77
Q6	100	30	-3.99
Q7	100	30	6.39
Q8	100	30	-4.58
Q9	100	30	8.43
Q10	100	30	-11.81
Q11	100	30	6.33
Solenoid-1	150	25	1.69
Solenoid-2	150	25	2.26
Buncher-1	300	20	120
Buncher-2	300	20	120
Buncher-3	300	20	120
Buncher-4	300	20	120
Buncher-5	445	20	146
Buncher-6	445	20	404

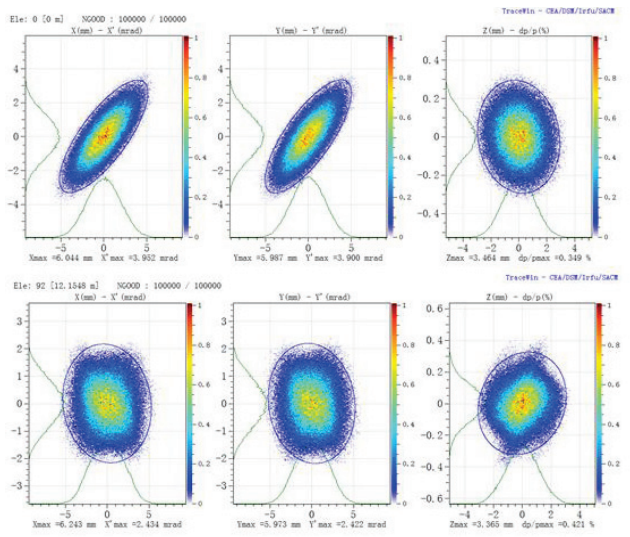

Figure 3: Distributions in the phase spaces in the MEBT2 (100000 particles, the upper plots are for the entrance and the lower plots for the exit).

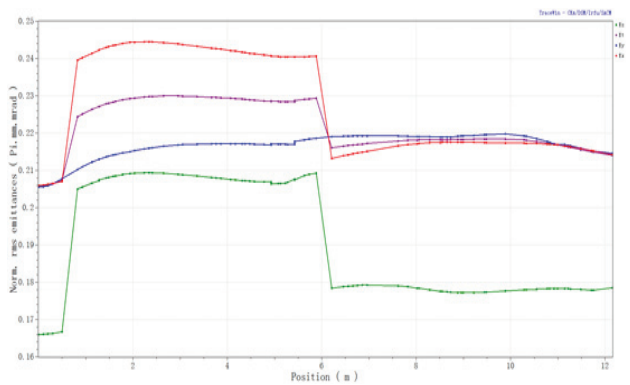

Figure 4: Emittance evolutions in the MEBT2.

The rms emittance evolution along the MEBT2 is shown in Figure 4. The emittance growth is about 4% in both transverse planes and 7.5% in the longitudinal phase. However, we can see significant increases in the halo emittance, especially in the 100% emittance (about 50%). This can be explained by the fact that in this non-periodic transfer section the beam halo is mismatched although the beam core is well matched. Different focusing and matching methods have been studied, but it looks that we have to bear the growth in the halo emittance [4].

OPERATING THE TWO INJECTORS IN PARALLEL MODE

When the two injectors are operated in the mode of one as the hot spare of the other, we need to consider how to define the hot standby mode. For the moment, we are

ISBN 978-3-95450-118-2

considering to operate the standby injector with all elements turned on but with a beam in a much reduced repetition rate, and to send the beam to the relevant beam dump. By doing so, we can monitor the status of the injector. When the central control system issues a command to switch between the injectors, e.g. from Injector-I to Injector-II, the beam at Injector-I is turned off. In the following, the polarities of all the three bending magnets in the MEBT2 are reversed. Then the beam at injector-II is turned to the CW mode. The time between the beam switch-off and switch-on will be within a few seconds, say less than five seconds. After the problem in Injector-I is solved, the injector will be tested with beams from low duty factor to CW, then it will be operated in the standard hot standby mode.

CONCLUSIONS

A self-consistent design for the beam transport line connecting two parallel injectors to the main linac has been designed for the C-ADS linac. It meets the requirements of achromatism, low emittance growth and hot-spare working mode, etc. A special design of using symmetrically-arranged bunchers in the bending section to obtain achromatism is proposed, and the algorithm is given. Multi-particle simulations including space charge effects show that the rms emittance growth is under control, about 10% or lower, but the growth in halo emittance is significantly larger.

Further optimizations are needed to include collimators and beam diagnostics,

REFERENCES

[1] Jingyu Tang, Zhihui Li et al., Conceptual Physics Design on the C-ADS Accelerators, IHEP-CADS-Report/2012-01E.
[2] J Staples, D Oshatz, T Saleh, Design of the SNS MEBT, 2000 Linac Conference, Monterey.
[3] D. Uriot, Manual for TraceWin.
[4] F. Gerigk, Space charge and beam halos in proton Linacs. Proc. of the 2002 Joint USPAS-CAS-Japan-Raussia Accelerator School, 2002, P257-288.

ISBN 978-3-95450-118-2